Chapter 5

Simulation results in unmagnetized plasmas

Numerous unique types of electrostatic and electromagnetic waves and instabilities exist in dusty plasmas because of the dust charging process. One such new mode is the dust charge fluctuation mode which is described in chapter 4. It has also been shown that dust charging typically introduces collisionless damping on wave modes in dusty plasmas. Another important prediction of the effects of dust charging is the production of plasma instabilities. These are streaming instabilities in which either the inertial charged dust fluid streams with respect to the background plasma, the inertial ion fluid drifts against the stationary dust grains and electrons, or the inertial electron fluid streams with respect to stationary ions and charged dust particulates. The mechanism for the instability arises because a dusty plasma with dust charge fluctuations behaves as a dissipative system. The damping of wave modes arises because of the phase difference between the total perturbed dust charge density and the wave potential. In this chapter, we investigate the unique streaming instability of ion acoustic waves due to dust charging effects. It has been proposed that such an instability may have important applications to laboratory and space plasmas. We used the same simulation model in this study that is an extention of previous chapter. The model was previously used to investigate charging effects on ion waves in magnetized dusty plasmas. We now describe the main features of our physical model used for studying streaming instabilities in unmagnetized dusty plasmas.

5.1 Theory

We consider ion acoustic waves generated by the streaming of the ion fluid relative to the dust with a speed v_{d}. The following dispersion relation can be obtained by assuming that the effects due to dust inertia are ignored ($\omega_{\mathrm{pd}} \rightarrow 0$), and considering waves in the ion acoustic frequency range ($\chi_{\mathrm{e}} = 1/k^2\lambda_{\mathrm{De}}^2, \chi_{\mathrm{i}} = -\omega_{\mathrm{pi}}^2/(\omega - v_{\mathrm{d}})^2$), equation (4.7) may be reduced to [*Jana et al.*, 1993]

$$(\bar{\omega}^2 - k^2C_{\mathrm{s}}^2)(\omega + i\eta) = -i\beta\left(1 - \frac{n_{\mathrm{e0}}}{n_{\mathrm{i0}}}\right)k^2C_{\mathrm{s}}^2. \tag{5.1}$$

Here ω_{pd} is the dust plasma frequency, $\bar{\omega} = \omega - kv_{\mathrm{d}}$, $C_{\mathrm{s}} = \lambda_{\mathrm{De}}\omega_{\mathrm{pi}}$ is the ion acoustic speed, ω_{pi} is the ion plasma frequency, λ_{De} is the electron Debye length, and n_{e0} and n_{i0} are the equilibrium electron and ion density. The parameter η and β are the dust charge fluctuation relaxation rate and the dust charge fluctuation damping rate [*Jana et al.*, 1993] and are given by

$$\eta = \frac{e|I_{\mathrm{e0}}|}{C}\left(\frac{1}{kT_{\mathrm{e}}} + \frac{1}{kT_{\mathrm{i}} - e\phi_{\mathrm{f0}}}\right) \tag{5.2}$$

and

$$\beta = \frac{|I_{\mathrm{e0}}|}{e}\frac{n_{\mathrm{d0}}}{n_{\mathrm{e0}}} \tag{5.3}$$

respectively, where e is the unit charge, I_{e0} is the equilbrium electron current, ϕ_{f0} is the equilibrium floating potential, and n_{d0} is the equilibrium dust density. We first consider the limit $v_{\mathrm{d}} = 0$. The dispersion relation (5.5) gives three roots corresponding to damped ion acoustic modes and purely damped dust cahrge fluctuation mode. The dust charge fluctuation mode has the approximate dispersion relation given by

$$\omega \approx i\eta \tag{5.4}$$

while the damped ion acoustic waves has the dispersion relation

$$\omega \approx kC_{\mathrm{s}} - i\frac{\beta}{2}\left(1 - \frac{n_{\mathrm{e0}}}{n_{\mathrm{i0}}}\right). \tag{5.5}$$

Therefore damping of ion acoustic waves depends on the damping constant β as well as the relative electron and ion densities. For significant damping the dust must carry most of the negative plasma charge. Next, we consider the case when $v_{\mathrm{d}} \neq 0$. Solving the dispersion relation (5.5) analytically in this case gives the approximate root for the ion acoustic waves as

$$\omega \approx k(v_{\mathrm{d}} - C_{\mathrm{s}}) + i\frac{\beta}{2}(1 - n_{\mathrm{e0}}/n_{\mathrm{i0}})\frac{C_{\mathrm{s}}}{v_{\mathrm{d}} - C_{\mathrm{s}}}. \tag{5.6}$$

It can be seen in this case that the free energy due to the drifting ions actually leads to growth of the ion acoustic waves if $v_{\mathrm{d}} > C_{\mathrm{s}}$. This effect is solely due to dust charging as the growth rate depends on the damping constant β. If $v_{\mathrm{d}} < C_{\mathrm{s}}$ the ion acoustic waves are damped. It should be noted for significant growth $n_{\rm i0} \gg n_{\rm e0}$. Figure 5.1 shows the damping rate variation of ion acoustic wave with $\tilde{\beta}$ for $\tilde{\eta} = 0.001$, 0.05 and 0.1. This agree well with equation (5.9). Figure 5.2 shows the dispersion relation of the ion acoustic waves for $\tilde{\eta} = \eta/\omega_{\rm pi} = 0.01$, $\tilde{\beta} = \beta/\omega_{\rm pi} = 0.01$, $\tilde{v}_{\rm d} = v_{\rm d}/C_{\rm s} = 1.5$, and $n_{\rm e0}/n_{\rm i0} = 0.1$. The growth rate $\omega_{\rm i}$ is essentially independent of wavenumber $k\lambda_{\rm De}$ in this regime. Figure 5.3 shows the growth rate variation with $\tilde{\beta}$ for $\tilde{\eta} = 0.001$, 0.05 and 0.1. Consistent with our previous work [*Chae et al.*, 2000], the growth rate decreases by increasing $\tilde{\eta}$ because large $\tilde{\eta}$ is expected to inhibit the lifetime of dust charge fluctuations which in turn results in less growth of the ion waves. Figure 5.4 shows the growth rate variation with $\tilde{v}_{\rm d}$ for $\tilde{\beta} =$ 0.0001, 0.001 and 0.01. Note that increasing $\tilde{\beta}$ increases the growth rate of the waves for $\tilde{v}_{\rm d} > 1$. Also an increase in $\tilde{\beta}$ may actually increase the critical drift velocity above $C_{\rm s}$.

5.2 Results

The numerical simulation model described in chapter 3 has been utilized to investigate the ion acoustic streaming instability. All numerical simulations are initialized charge neutral with the number of positive and negative charges equal, that is, $en_{\rm e0} + Q_{\rm d0}n_{\rm d0} = en_{\rm i0}$. All dust grains are initialized with $I_{\rm e0} + I_{\rm i0} = 0$ which determines the equilibrium grain charge in the absence of perturbations. A reduced electron-ion mass ratio of $m_{\rm e}/m_{\rm i} = 10^{-2}$ is used to resolve the electron and ion timescales in a reasonable amount of computational time. We also choose $\frac{Q_{\rm d}}{m_{\rm d}}\frac{q_{\rm i}}{m_{\rm i}} \approx 10^{-6}$ which implies the dust doesn't move significantly during the time period of the simulation for simplicity. The simulation box used is 128×128 grid cells. In the following results, all dust grains are initalized with the same mass $m_{\rm j}$ for simplicity. To study the streaming instability, we initialize the simulation with a weak 0.5% ion density perturbation $\tilde{n}_{\rm i}$ and the electron density perturbation $\tilde{n}_{\rm e}$ is calculated with $\tilde{n}_{\rm e} = \tilde{n}_{\rm i}/(1 + k^2\lambda_{\rm De}^2)$ to be consistant for ion acoustic waves [*Chen*, 1998]. The perturbations are then given by

$$n_{\mathrm{i}}(x, y, t = 0) = n_{\mathrm{i0}}(1 + 0.005 \cos(k_{\mathrm{x}} x)) \tag{5.7}$$

$$n_{\mathrm{e}}(x, y, t = 0) = n_{\mathrm{e0}} \left(1 + 0.005 \frac{\tilde{n}_{\mathrm{e}}}{\tilde{n}_{\mathrm{i}}} \frac{n_{\mathrm{i0}}}{n_{\mathrm{e0}}} \cos(k_{\mathrm{x}} x)\right) \tag{5.8}$$

where $k_{\mathrm{x}} = \frac{2\pi m}{L}$, $\lambda_{\mathrm{De}} = 1$, and $m = 8$ for mode 8 used here. Also, we chose $\tilde{n}_{\mathrm{d}} = \tilde{Q}_{\mathrm{d}} = 0$ initially. In this case, we use 9 simulation dust particles per cell with an equilibrium dust charge $Q_{\mathrm{d0}} = 10000$ electrons which gives a dust charge density of 90% of the background equilibrium ion charge density for the chosen value of n_{i0}. We choose $q_{\mathrm{s}} = 116$ as the production rate.

Figure 5.5 shows the temporal damping of ion acoustic oscillation potential, ion density and dust charge fluctuations. Figure 5.6 shows the initial ($\omega_{\mathrm{pi}} t = 0$) density perturbations spatially of each species for $\tilde{v}_{\mathrm{d}} = 1.5$ as well as the perturbations at the end of the simulation ($\omega_{\mathrm{pi}} t = 60$). Note that well defined perturbations in the dust charge as well as plasma densities are produced by the streaming instability. Figure 5.7 and Figure 5.8 show the ion density perturbations and dust charge fluctuations for the case in which $\tilde{v}_{\mathrm{d}} = 0.5$ and $\tilde{v}_{\mathrm{d}} = 1.5$ with the parameter $\tilde{\beta} = 0.0$ and 0.01. These clearly exibit damping and growth of the ion acoustic waves. The calculated simulation damping and growth rate are 0.007 and 0.005, respectively, which agree quite well with the theoretical estimation in Figure 5.5 of 0.009. It is noted that the growth of the ion acoustic waves is associated with growth of the dust charge fluctuations from Figure 5.8. Figure 5.9 shows the frequency spectrum of the ion density perturbations $|n_{\mathrm{i}}(\omega)|^2$ for each case calculated by using Fast Fourier Transforms FFTs. This clearly shows the damping and growth of the waves at frequency $\omega/\omega_{\mathrm{pi}} = 0.2$ which is the frequency of the ion acoustic waves for $\tilde{v}_{\mathrm{d}} = 0.5$ and $\tilde{v}_{\mathrm{d}} = 1.5$ described in equation (5.8) for our parameters.

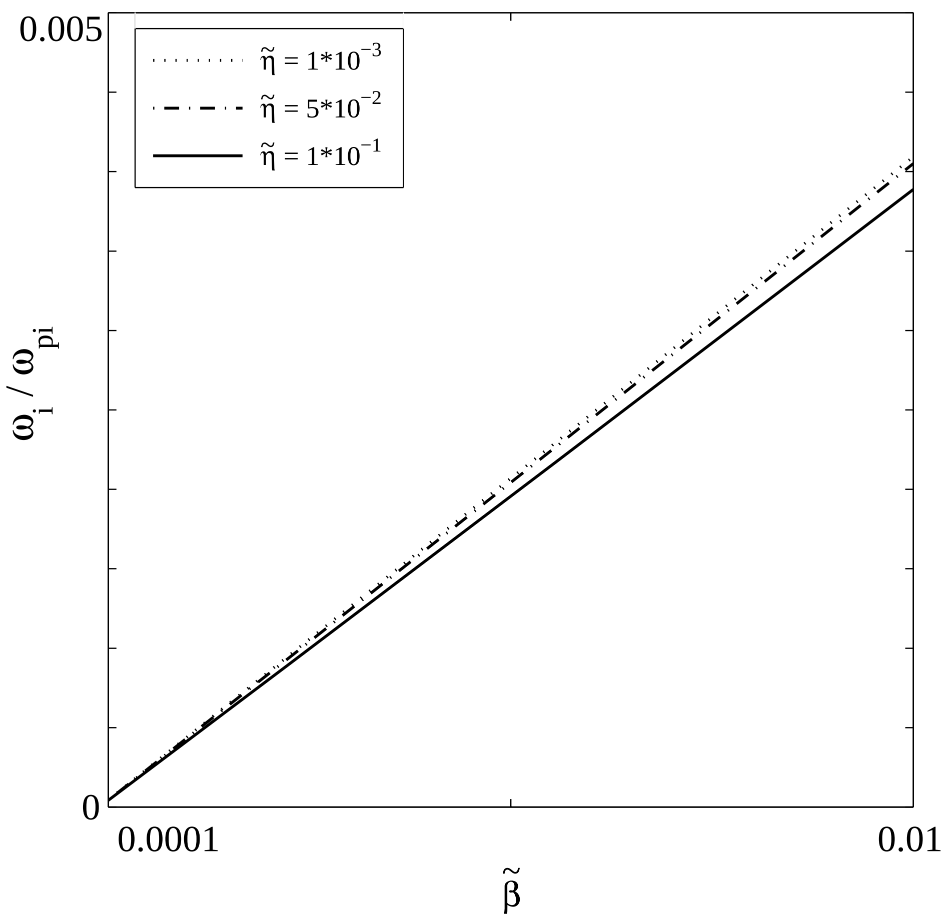

Figure 5.1: Damping rate $\omega_{\rm i}$ vs $\tilde{\beta}$ for $\tilde{\eta}$=0.001, $\tilde{\eta}$=0.05, and $\tilde{\eta}$=0.1 for ion acoustic waves.

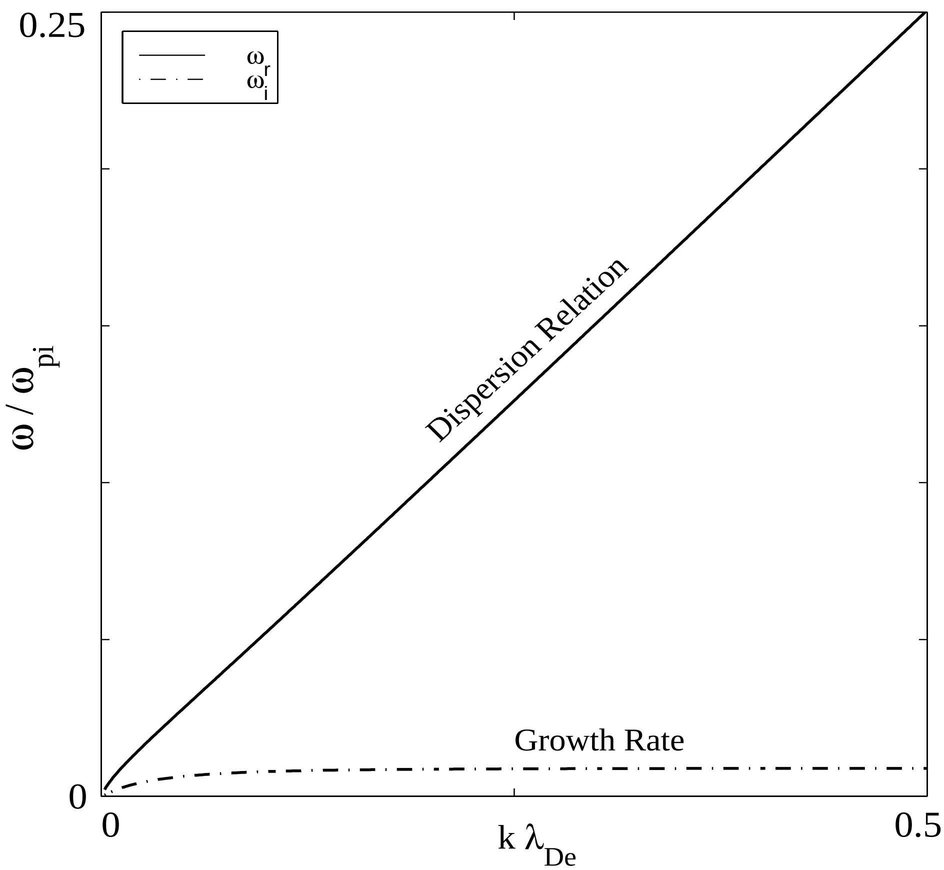

Figure 5.2: Dispersion relation and growth rate for the ion acoustic streaming instability due to dust charge fluctuations.

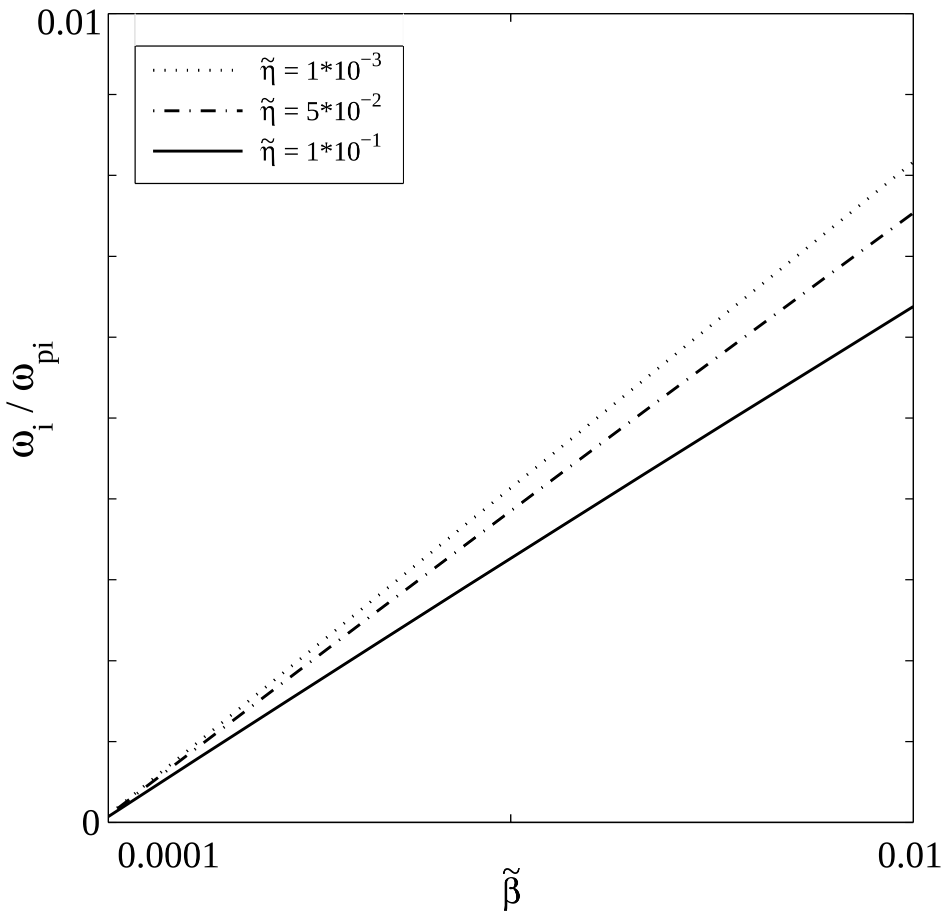

Figure 5.3: Growth rate $\omega_{\rm i}$ vs $\tilde{\beta}$ for $\tilde{\eta}$=0.001, $\tilde{\eta}$=0.05, and $\tilde{\eta}$=0.1 for the ion acoustic streaming instability.

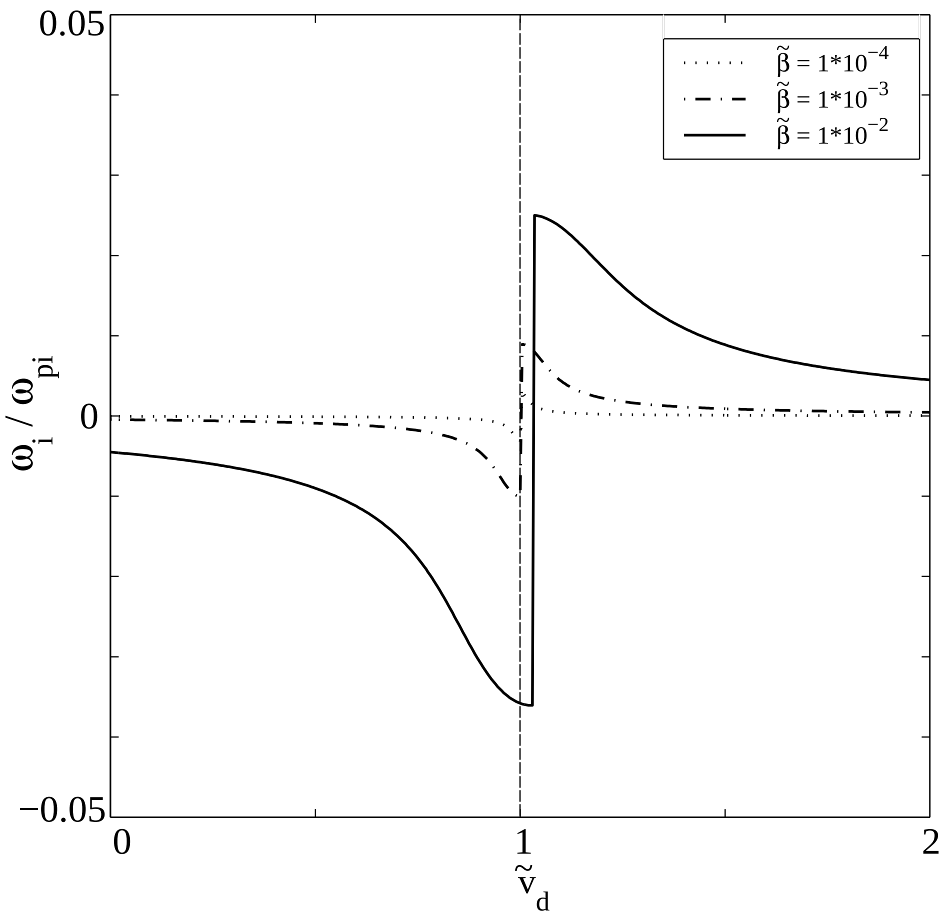

Figure 5.4: Growth rate $\omega_{\rm i}$ from equation (12) for ion acoustic waves showing growth for $\tilde{v}_{\rm d} = v_{\rm d}/C_{\rm s} > 1$ and damping for $\tilde{v}_{\rm d} = v_{\rm d}/C_{\rm s} < 1$.

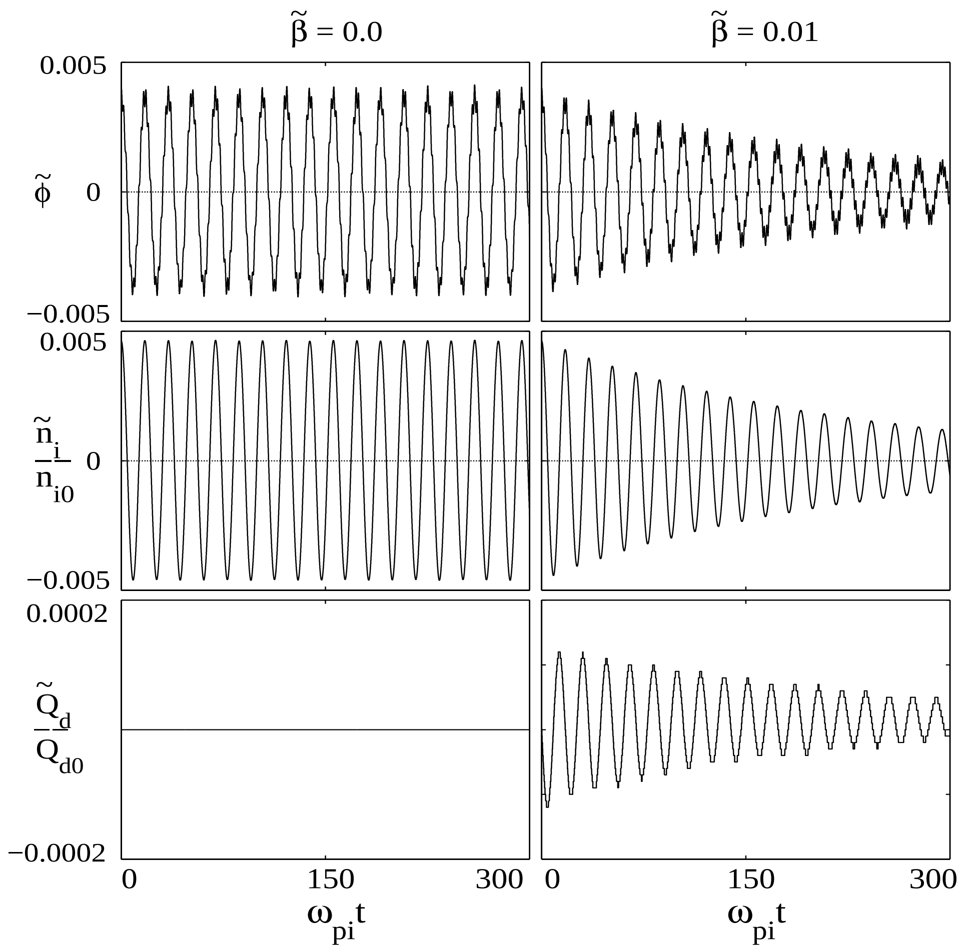

Figure 5.5: Temporal damping of ion acoustic oscillation potential, ion density, and dust charge fluctuations. $\tilde{\eta} = 1.0$.

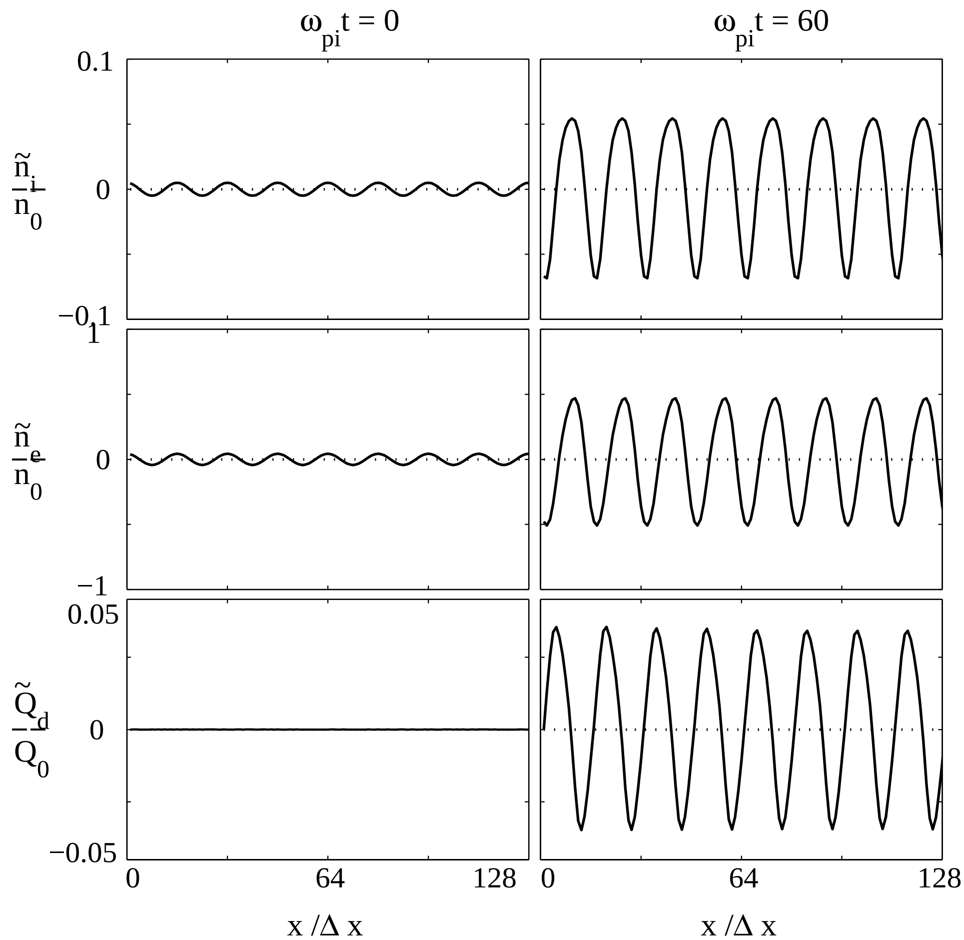

Figure 5.6: Ion and electron densities and dust charge with $\tilde{\beta} = 0.01$ for ion acoustic streaming instability for $\tilde{v}_{\rm d} = 1.5$ at $\omega_{\rm pi}t = 0$ and $\omega_{\rm pi}t = 60$.

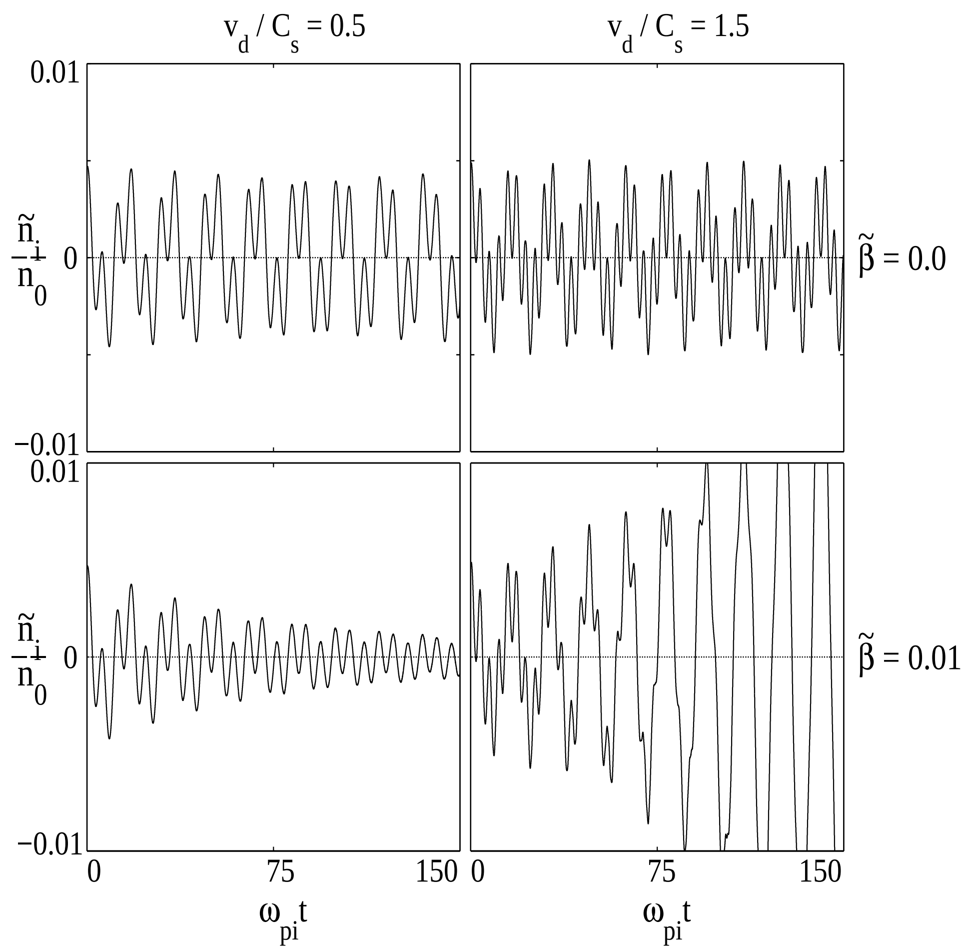

Figure 5.7: Numerical simulation of the ion acoustic streaming instability due to dust charge fluctuations. For $\tilde{v}_{\rm d} = 0.5$ ion acoustic waves are damped. The instability produces growth in ion acoustic waves for $\tilde{v}_{\rm d} = 1.5$.

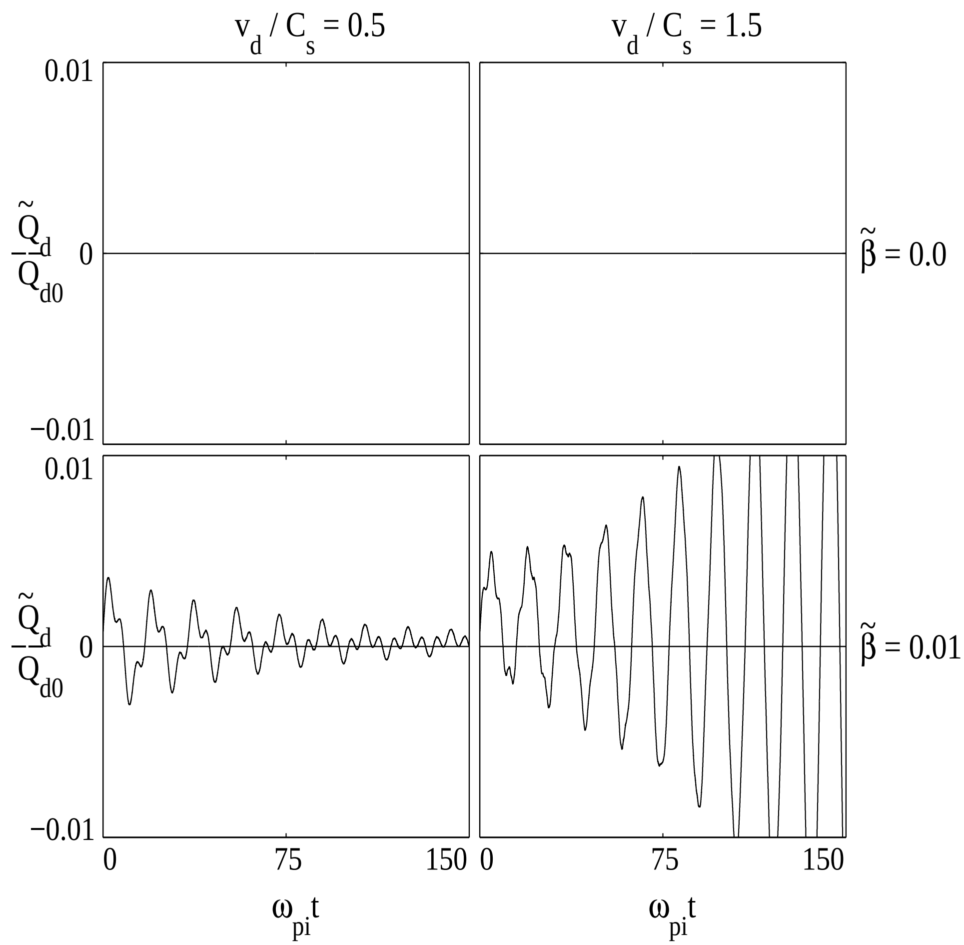

Figure 5.8: Numerical simulation of the ion acoustic streaming instability due to dust charge fluctuations. Note damping and growth of dust charge fluctuations for $\tilde{v}_{\mathrm{d}} = 0.5$ and $\tilde{v}_{\mathrm{d}} = 1.5$, respectively.

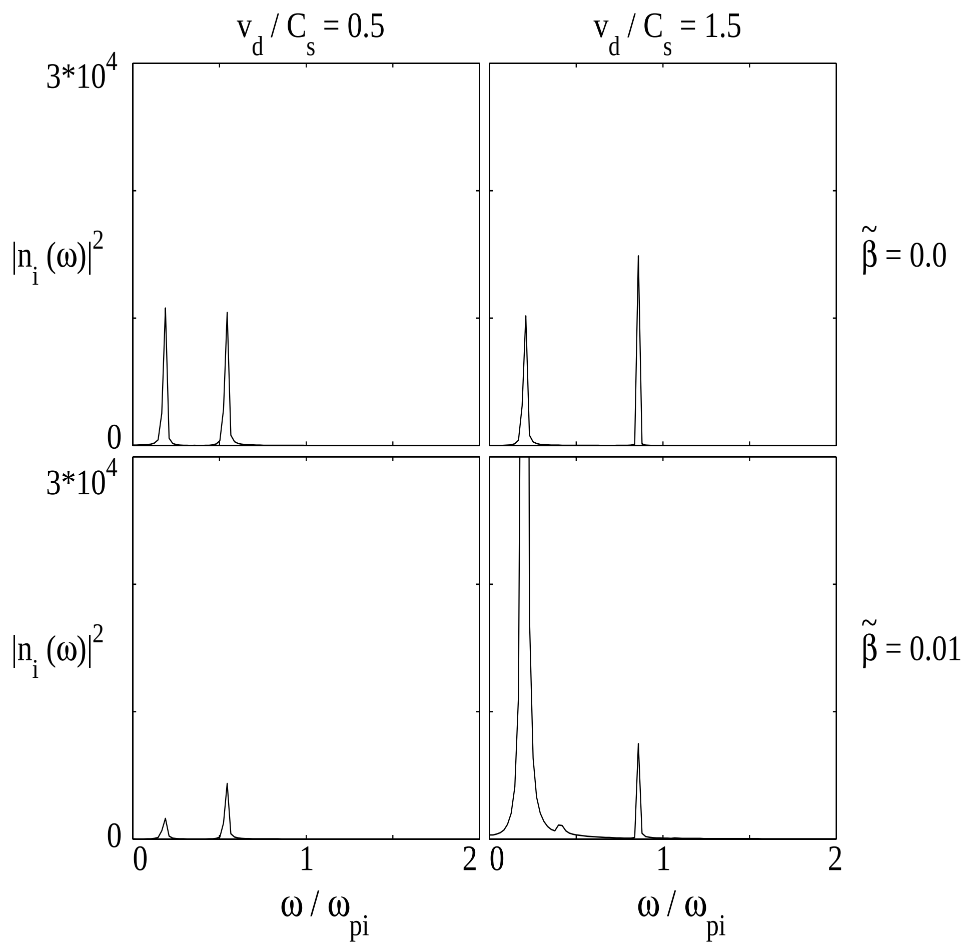

Figure 5.9: Ion density power spectrum of the ion acoustic streaming instability. The waves of frequency $\omega/\omega_{\rm pi} = 0.2$ damp for $\tilde{v}_{\rm d} = 0.5$ and grow for $\tilde{v}_{\rm d} = 1.5$.